Multiple Frontal Structures in the Baiu Frontal Zone Observed by Aircraft on 27 June 2004

Qoosaku Moteki[1], Taro Shinoda[2], Shingo Shimizu[3], Shinichiro Maeda[2], Haruya Minda[2], Kazuhisa Tsuboki[2], and Hiroshi Uyeda[1, 2]

[1]*Institute of Observational Research for Global Change, Japan Agency for Marine-Earth Science and Technology, Yokosuka, Japan*

[2]*Hydrospheric Atmospheric Research Center, Nagoya Universiy, Nagoya, Japan*

[3]*National Research Institute for Earth Science and Disaster Prevention, Tsukuba, Japan*

Abstract

The structure of the Baiu frontal zone over the East China Sea on 27 June 2004 was investigated using data from aircraft observations. During the period of 09–12 JST (Japanese Standard Time: UTC + 9 hours), three cloud zones appeared over the East China Sea. The Baiu frontal zone is conveniently divided into three zones on the basis of the three cloud zones. The zones on the southern side, in the middle, and on the northern side are called FZ1, FZ2, and FZ3, respectively. The position of FZ2 corresponded with that of a stationary front on the surface weather map. Remarkable variations of winds, potential temperature, and moisture corresponding to the three zones were detected using *in situ* measurements at 500 m MSL (Mean Sea Level). In FZ1, a decreased southerly wind area associated with a remarkable moisture gradient was seen, although the potential temperature gradient was unclear. FZ2 had remarkable gradients of potential temperature and moisture associated with a drastic change from southwesterly to northwesterly winds. FZ3 also had remarkable gradients of potential temperature and moisture. This study shows observational evidence of the fact that multiple frontal structures exist inside the Baiu frontal zone.

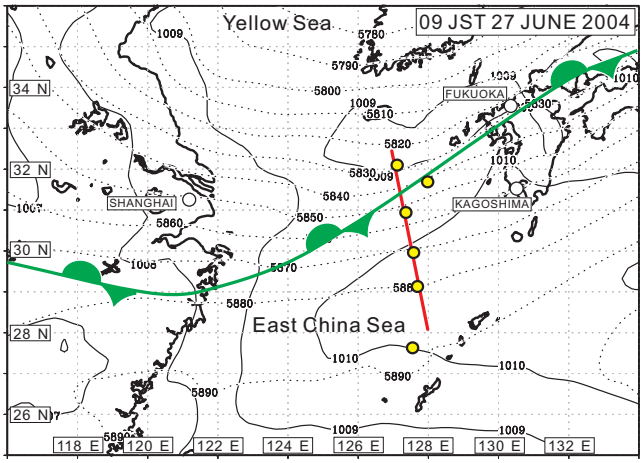

Fig. 1. Sea level pressure (solid contours) and geopotential height at 500 hPa (dotted contours) with RANAL at 09 JST on 27 June 2004. The red line is the track of the 500 m MSL flight of the G-II from 0852 to 0950 JST. Open yellow circles represent the locations of dropsondes. The position of the Baiu front is from the JMA weather map.

1. Introduction

The rainy season over the Japan Islands from June to July is called the Baiu season, and many strong rainfall events are induced in the Baiu frontal zone. The Baiu frontal zone is generally regarded as a low-level pressure trough between two high pressure air masses to the north and south. Moteki et al. (2004a, b: hereafter M2004) revealed that multiple distinct fronts existed in the Baiu frontal zone over the East China Sea using analyses with Doppler radar observations and a non-hydrostatic model. They demonstrated that two distinct fronts existed in the Baiu frontal zone: the Baiu front extending from the inland of China and the water vapor front forming over the East China Sea. The water vapor front is a convergence line with an oceanic southwesterly and a continental westerly flows in a warm and moist region to the south of the Baiu front. Based on the discovery of the water vapor front they emphasized that a inhomogeneous distribution of low-level moisture in a warm and moist region had a significant role on the formation of the precipitation system.

However, it is difficult to analyze accurately the inhomogeneous moisture distribution in the initial condition for numerical predictions (Kato et al. 2003; Kato and Aranami 2005) because operational observation points are very few over the East China Sea. Understanding of the fine-scale structure of the Baiu frontal zone over the East China Sea and the inhomogeneous moisture distribution to the south is strongly required in order to consider the future operational observation strategy.

M2004 proposed a field experiment using an aircraft to observe the fine-scale structure of the Baiu frontal zone over the East China Sea using *in situ* measurements and dropsondes. Four flights in total were conducted in the 2004 and 2005 Baiu seasons, and high-quality data were successfully obtained. This paper describes a case on 27 June 2004 which is suitable for clarifying the multiple frontal structures in the Baiu frontal zone. The objective of this study is to reveal multiple frontal structures of the Baiu frontal zone over the East China Sea using data from aircraft observations.

2. Design of aircraft observations

The aircraft Gulfstream-II (hereafter called by G-II) used for the observations was at Kagoshima airport during the period of 23–27 June in 2004. A visual flight with G-II is possible from 06 JST (Japanese Standard Time) to 19 JST. *In situ* measurements for pressure, temperature, dew point temperature, horizontal winds and vertical winds at 500 m MSL and dropsonde observations at 6 locations were conducted on 27 June.

Corresponding author: Qoosaku Moteki, Institute of Observational Research for Global Change (IORGC), Japan Agency for Marine-Earth Science and Technology, 2-15 Natsushima, Yokosuka 237-0061, Japan. E-mail: moteki@jamstec.go.jp.

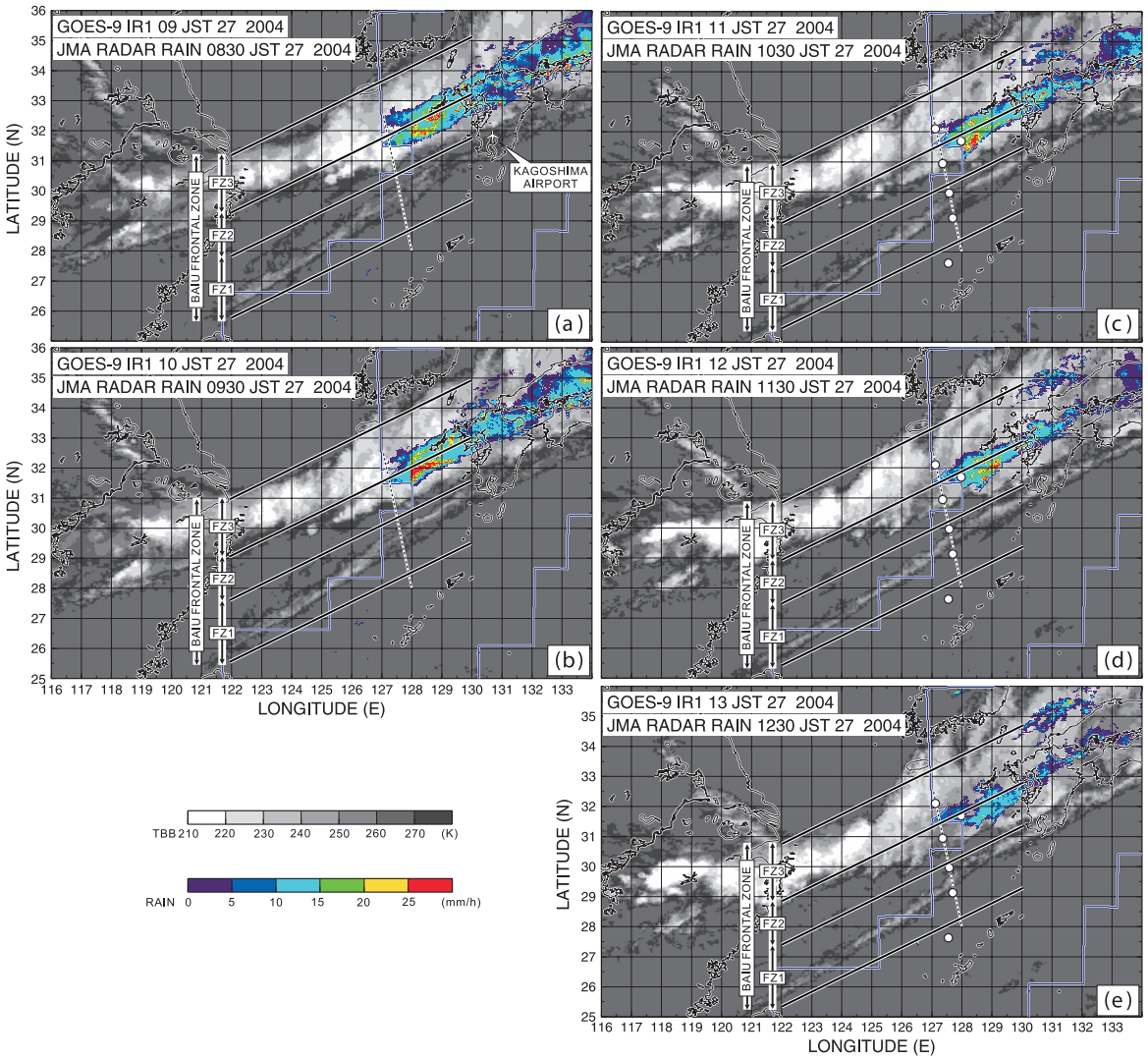

Fig. 2. Infrared satellite images (gray shading) at (a) 09, (b) 10, (c) 11, (d) 12, and (e) 13 JST on 27 June 2004. Rainfall intensity distributions (color shading) at 0830, 0930, 1030, 1130, and 1230 JST are superimposed onto (a), (b), (c), (d), and (e), respectively. The black solid lines show conveniently defined boundaries of FZ1, FZ2, and FZ3. The blue solid lines show the boundaries of the observation area of the JMA radar. The dashed line is the track of the 500 m MSL flight of the G-II from 0852 to 0950 JST. The open circles in (c), (d), and (e) represent the locations of dropsondes. The location of Kagoshima airport is indicated by the airport symbol in (a).

A suitable flight path and takeoff time were determined using the forecast results provided by the Japan Meteorological Agency (JMA) Regional Spectral Model (RSM, Numerical Prediction Division/JMA, 2002) and the Cloud Resolving Storm Simulator (CReSS, Tsuboki and Sakakibara 2002) nested within the RSM. A horizontal grid size of 5 km, horizontal grid points of 213 × 303, vertical levels of 38, and the cold rain process apply to the predictions with CReSS.

3. Overview of the synoptic situation

The fields of the sea level pressure and geopotential height at 500 hPa with the JMA regional analysis (RANAL, Numerical Prediction Division/JMA 2002) at 09 JST on 27 June 2004 are shown in Fig. 1. Over the East China Sea, a pressure trough at the surface associated with the Baiu front extends in the east-west direction. A weak trough at 500 hPa extending from the Yellow Sea to inland China is seen in the north of the Baiu frontal zone.

Under such environmental conditions, active convections developed over the East China Sea from 09 to 13 JST. Figure 2 shows infrared satellite images obtained with the Geostationary Operational Environmental Satellite (GOES-9) and rainfall intensity distributions obtained with the JMA radars. Three cloud zones are found to form over the East China Sea. In this study, the zone with a north-south width of about 500 km including the three cloud zones is called the Baiu frontal zone. The Baiu frontal zone is conveniently divided into three zones on the basis of the three cloud zones. Here, the zones on the southern side, in the middle, and on northern side are called FZ1, FZ2, and FZ3, respectively. The boundaries between the three zones are determined on the basis of the cloud distribution at 10 JST, in which three cloud zones are clearly seen. The boundaries at 09 JST and 11–13 JST are shifted from those at 10 JST considering a southward motion.

The cloud zone in FZ1 during the flight observation period has no precipitation. In FZ1, only clouds in the middle troposphere were confirmed with a visual observation from the G-II. The cloud zone in FZ2 extends

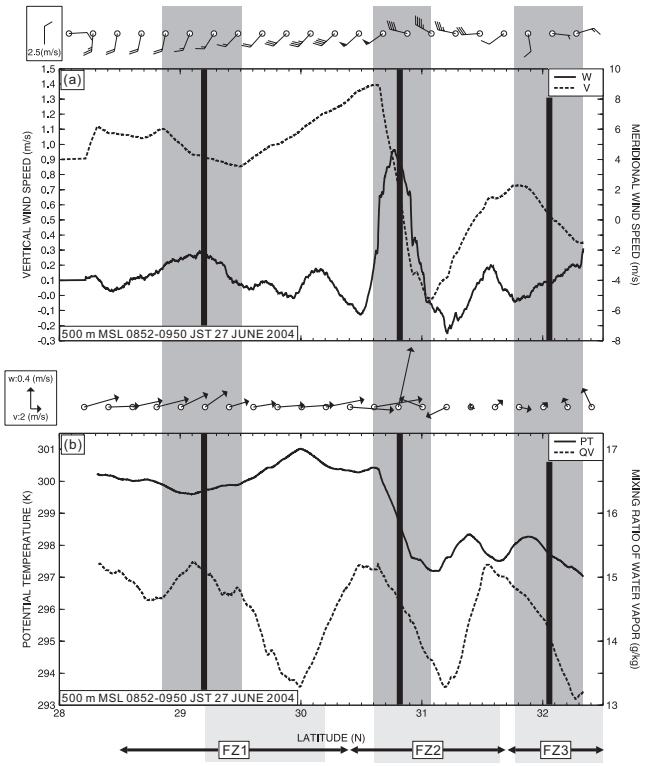

Fig. 3. Flight-level data from the G-II as it penetrated the Baiu frontal zone at 500 m MSL along the pass shown in Fig. 1. (a) The vertical velocity (solid line), meridional wind velocity (dashed line), and horizontal winds (barb) are plotted. The pennant, full barb, and half barb represent 12.5, 2.5, and 1.25 m s^{-1}, respectively. (b) Potential temperature (solid line), mixing ratio of water vapor (dashed line), and vectors with meridional and vertical winds. The light-shaded areas in the bottom of the figure correspond to the cloud zones of FZ1, FZ2, and FZ3. The dark-shaded areas represent the convergence zones of the meridional component. The positions of the inflection point of meridional wind velocity are indicated by bold solid lines.

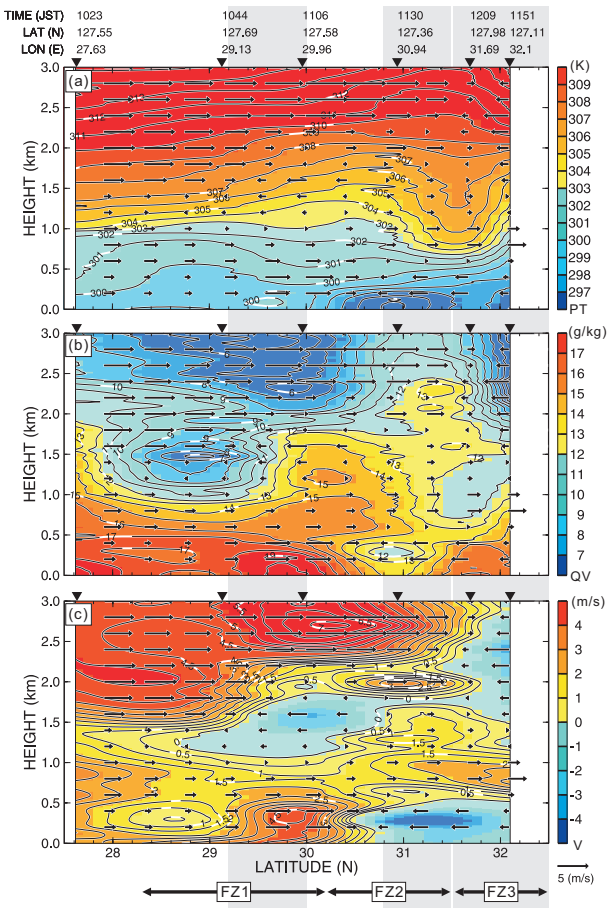

Fig. 4. Vertical cross sections based on dropsonde data. (a) Potential temperature (color shading and contoured every 1 K), (b) mixing ratio of water vapor (color shading and contoured every 1 g kg^{-1}), and (c) meridional wind speed (color shading and contoured every 0.5 m s^{-1}). The times and locations of the dropsonde observations are shown at the top of the figure. The light-shaded areas at the bottom of the figure correspond to the cloud zones of FZ1, FZ2, and FZ3. Vectors indicate meridional winds.

Table 1. Horizontal gradients of potential temperature (K per 100 km) and mixing ratio of water vapor (g kg^{-1} per 100 km) in the convergence zones of the meridional component corresponding to FZ1, FZ2, and FZ3.

	FZ1	FZ2	FZ3
ΔPT		6.4	3.0
Δq_v	1.7	3.0	3.2

from the central part of the East China Sea to the east-northeast. From 0830 to 1130 JST, the cloud zone in FZ2 is associated with a strong precipitation area (128–129 E) more than 25 mm h^{-1}, and the precipitation in FZ2 decays after 1230 JST. The location of the Baiu front at 09 JST on 27 June analyzed with the JMA weather map (Fig. 1) corresponded to that of FZ2. A cloud zone in FZ3 extends from the east coast of the Chinese continent. From 0930 to 1030 JST, the cloud zone is associated with a moderate precipitation area of 15–20 mm h^{-1}, and the precipitation in FZ3 decays after 1130 JST.

4. *In situ* measurement analysis

In situ measurements of meteorological elements at 500 m MSL were conducted from 0852 to 0950 JST, and the features of FZ1, FZ2, and FZ3 were detected (Fig. 3). Variables of the *in situ* data were recorded at a frequency of 10 Hz. A running mean in which spatial scales less than about 20 km (smaller than a convective scale) were removed was applied to the data used here.

The three zones of FZ1, FZ2, and FZ3 are characterized by remarkable wind shifts and peaks with upward velocity (Fig. 3a). In FZ1, the speed of the southerly winds decreases by about 2 m s^{-1}, and a vertical velocity of about 0.3 m s^{-1} is seen near the inflection point of meridional velocity. In FZ2, a change from southerly winds of about 9 m s^{-1} to northerly winds of about 5 m s^{-1} and a vertical velocity of about 1 m s^{-1} are seen near the inflection point of meridional velocity. In FZ3, a change from southerly winds of about 2 m s^{-1} to northerly winds of about 1 m s^{-1} and a vertical velocity of about 0.3 m s^{-1} are seen on the northern side of the inflection point of meridional velocity.

Significant features of the three frontal zones are also seen in the variations of potential temperature PT and mixing ratio of water vapor q_v (Fig. 3b). There are two potential temperature drops and three peaks of the mixing ratio of water vapor. To quantify the variations corresponding to the three frontal zones, the horizontal gradients of PT and q_v are calculated using the maximum and minimum values in each convergence zone of the meridional component (Table 1). FZ1 has almost no significant PT gradient but has a q_v gradient of about

1.7 g kg^{-1} per 100 km. FZ2 has the largest PT gradient of about 6.4 K per 100 km in the three frontal zones and a q_v gradient of about 3.0 g kg^{-1} per 100 km. FZ3 has a PT gradient of about 3.0 K per 100 km and a q_v gradient of about 3.2 g kg^{-1} per 100 km.

The features of FZ1 are very similar to the water vapor front shown by M2004: a remarkable q_v gradient in southerly wind field associated with a remarkable wind shift and no PT gradient. It cannot be concluded whether FZ1 is the water vapor front or not from the 1-dimensional data alone. However, the existence of FZ1 itself provides evidence that the q_v distribution in the southerly wind field is not homogeneous. Although FZ1 had no precipitation area, remarkable variations of wind and moisture in FZ1 could affect the process of water vapor supply to precipitation areas in FZ2 and FZ3.

5. Dropsonde analysis

Dropsonde observations from 12 km MSL at 6 locations were conducted from 1023 to 1209 JST (their locations are shown in Figs. 2c, d, and e). To describe the vertical structure of the Baiu frontal zone, the dataset interpolated with a meridional 0.1 degree-grid interval and a 10 m-grid interval in vertical is provided from the dropsonde data.

As shown in analyses of *in situ* measurements, a horizontal gradient of PT below 1 km in FZ1 is unclear (Fig. 4a). In the zone between 2 dropsonde locations at 27.63 and 29.13 degrees north, the depth of a high q_v air mass (> 12 g kg^{-1}) becomes shallow to the north (Fig. 4b), and the southerly wind speed slows down below 1 km (Fig. 4c). At heights of 1–1.5 km MSL, a layer of weak northerly winds that extends from the northern part of the Baiu frontal zone is seen, and the southern edge of the layer is found to correspond to the location of FZ1.

FZ2 is found to correspond to the southern edge of a cold air mass less than 299 K with northerly winds (Figs. 4a and c). A high q_v air mass (> 12 g kg^{-1}) rises up over the cold air (Fig. 4b).

The cold air becomes deep to the north, and the PT gradient in the layer of 0.5–1 km MSL is remarkable in FZ3. Although FZ3 is in the cold air, a relatively large q_v value of about 15 g kg^{-1} is seen below 0.5 km MSL.

The vertical structure of the Baiu frontal zone revealed here strongly supports the idea that multiple distinct fronts existed in the Baiu frontal zone over the East China Sea shown by M2004. However, there are some differences between the cases shown by M2004 and this study. Weak northerly winds in the 1–1.5 km MSL layer are not seen in M2004, which does not have the structure of FZ3 in cold air.

6. Summary and conclusions

The structure of the Baiu frontal zone over the East China Sea on 27 June 2004 was investigated using data from aircraft observations. According to the RANAL at 09 JST on 27 June, a pressure trough at the surface associated with the Baiu front extended in the east-west direction over the East China Sea, and a weak trough at 500 hPa was seen in the north of the Baiu frontal zone. During the period of 09–12 JST, three cloud zones appeared over the East China Sea. The Baiu frontal zone including the three cloud zones was divided into three zones, which were called FZ1, FZ2, and FZ3.

FZ1 corresponded to a decreased southerly wind area below 1 km MSL and the southern edge of northerly winds in the layer near 1.5 km MSL. At 500 m MSL, FZ1 was associated with a vertical velocity of about 0.3 m s^{-1} but no precipitation. The gradient of potential temperature in FZ1 was unclear, but that of the mixing ratio of water vapor was significant (about 1.7 g kg^{-1} per 100 km at 500 m MSL).

FZ2 corresponded to the southern edge of a cold air mass in association with northerly winds below 0.5 km MSL and was associated with a strong precipitation area of more than 25 mm h^{-1}. A stationary front analyzed on the surface weather map with the JMA corresponded to the position of FZ2. At 500 m MSL, FZ2 was associated with a vertical velocity of about 1 m s^{-1} and remarkable gradients of potential temperature and mixing ratio of water vapor (about 6.4 K per 100 km and 3.0 g kg^{-1} per 100 km).

FZ3 was associated with a moderate precipitation of 15–20 mm h^{-1} in cold air. At 500 m MSL, FZ3 was associated with a vertical velocity of about 0.3 m s^{-1}, and the remarkable gradients of potential temperature and mixing ratio of water vapor (about 3.0 K per 100 km and 3.2 g kg^{-1} per 100 km).

This study shows observational evidence of the fact that multiple frontal structures exist inside the Baiu frontal zone. Although FZ1 had no precipitation area, it could be very important in the Baiu frontal zone because the structure of FZ1 could affect the process of water vapor supply to precipitation areas in FZ2 and FZ3. It is considered that structures such as FZ1 need to be represented in the initial conditions for numerical models in order to make more accurate quantitative predictions of strong precipitation. Over the East China Sea, although adding operational observation points of upper-air sounding may be difficult, adding a surface weather station using ocean buoy, for example, could be very effective to detect the structure like FZ1.

Acknowledgments

We are grateful to the staff of Diamond Air Service, Co. Ltd. for operating G-II. The satellite image is from the weather satellite image archive of Kochi University (http://weather.is.kochi-u.ac.jp). This study was supported by a Grant-in-Aid for Scientific Research of the Japan Society for the Promotion Science.

References

Kato, T., M. Yoshizaki, K. Bessho, T. Inoue, Y. Sato and X-BAIU-01 observation group, 2003: Reason for the failure of the simulation of heavy rainfall during X-BAIU-01 – Importance of a vertical profile of water vapor for numerical simulation – *J. Meteor. Soc. Japan*, **81**, 993–1013.

Kato, T., and K. Aranami, 2005: Formation factors of 2004 Niigata-Fukushima and Fukui heavy rainfalls and problems in the predictions using a cloud-resolving model. *SOLA*, **1**, 1–4.

Moteki, Q., H. Uyeda, T. Maesaka, T. Shinoda, M. Yoshizaki and T. Kato, 2004a: Structure and development of two merged rainbands observed over the East China Sea during X-BAIU-99 Part I: Meso-β-scale structure and development processes. *J. Meteor. Soc. Japan*, **82**, 19–44.

Moteki, Q., H. Uyeda, T. Maesaka, T. Shinoda, M. Yoshizaki and T. Kato, 2004b: Structure and development of two merged rainbands observed over the East China Sea during X-BAIU-99 Part II: Meso-[alpha]-scale structure and build-up processes of convergence in the Baiu frontal region. *J. Meteor. Soc. Japan*, **82**, 45–65.

Numerical Prediction Division/Japan Meteorological Agency, 2002: Outline of the operational numerical weather prediction of the Japan Meteorological Agency. 158 pp. [Available from JMA, 1-3-4 Otemachi, Chiyoda-ku, Tokyo 100-8122, Japan.]

Tsuboki, K., and A. Sakakibara, 2002: Large-scale parallel computing of Cloud Resolving Storm Simulator. High Performance Computing, Springer, H. P. Zima et al. Eds, 243–259.

Manuscript received 7 July 2006, accepted 25 August 2006
SOLA: http://www.jstage.jst.go.jp/browse/sola/